

The high concentration and uniform distribution of diamond particles in Ni-diamond composite coatings by sediment co-deposition

Jiaqian Qin,^{a,b,*} Xinyu Zhang,^{b,*} Yannan Xue,^b Malay Kumar Das,^{a,c}
 Adisak Thueploy,^a Sarintorn Limpanart,^a Yuttanant Boonyongmaneerat,^a
 Mingzhen Ma^b and Riping Liu^b

Ni-diamond composite coatings with high concentration and uniform distribution of diamond particles were prepared by using sediment co-deposition (SCD) technique from Watts-type electrolyte without any additives. The surface and cross-section morphology was evaluated by optical microscope (OM) and scanning electron microscopy (SEM). It was demonstrated that the Ni-monolayer diamond composite coatings $\sim 40 \pm 5 \mu\text{m}$ was successfully prepared by the new developed setup for SCD technique. Using this new developed setup, high concentration and uniform distribution of diamond particles of Ni-monolayer diamond composite coatings were easily fabricated. The wear resistance and cutting performance of obtained composite coatings were also investigated. The results revealed that anti-wear and cutting performance is superior to those prepared via conventional co-electrodeposition (CED) technique and pure Ni coatings. In the SCD process, with the increasing diamond content, the wear resistance is approximately the same, and the cutting performance decreases. Therefore, not only the diamond particle content is responsible for the wear resistance and cutting performance, the distribution of diamond particles is also very important factor.

Copyright © 2014 John Wiley & Sons, Ltd.

Keywords: Ni-diamond composite coatings; electrodeposition; wear resistance; cutting performance

Introduction

Particle-reinforced metal matrix composites generally exhibit wide engineering applications as a result of their high hardness, good wear resistance, and corrosion resistance compared with pure metal or alloy.^[1] Owing to its relatively low operational cost and low processing temperature, the co-electrodeposition (CED) technique has been aggressively developed. During the process, the particles are suspended in a conventional plating electrolyte and captured into the growing metal coatings. Successful CED of micro-sized and nano-sized particles such as SiC,^[2–9] ZrO₂,^[7,10] Al₂O₃,^[7,11–13] Si₃N₄,^[14] diamond,^[15–17] etc. with metal or alloy have been reported by adopting CED technique.

It is well known that the properties of the composite coatings are heavily dependent on the degree of particle incorporation in the deposit. Higher incorporation percentages and more uniform distribution of inert particles in the metal matrix lead to the improvement of the mechanical, tribological, anti-corrosion, and anti-oxidation properties of the composite coatings. While, deposition coatings created using conventional CED technique have relatively low particle content.^[18] Hence, methods to improve the particle concentration in composite coatings have attracted much attention. Now, there are many methods to increase the content of the particles in the composite coatings, such as the addition of metal cationic accelerators^[19,20] and organic surfactants^[9,21] or the common method with increasing the particle concentration in the bath,^[22] the ultrasonic irradiation,^[23] and changing the type of applied current.^[24] Among these methods, use of anion, cation, and nonionic surfactants are used extensively to obtain more

incorporation of particles in composite coatings. However, excessive surfactants will reduce the cathode area and increase deposit brittleness.^[25] Increasing the particle concentration in the electrolyte undoubtedly increases the cost, especially for precious materials such as diamond particles.^[15–17]

Uniformly dispersed particles in the electrodeposition solution allow a continuous flux of particles to the cathode, where they can be adsorbed and eventually trapped within the growing metal matrix. A satisfactory long adsorption time is essential to the successful anchoring of the particles by the depositing metal.^[26,27] Earth's gravitational forces interfere with the dispersion and adsorption processes.^[28] Co-deposition in a reduced gravity environment would eliminate sedimentation. However, lower gravity environment will cause a lot. In 1972, a new technique called sediment

* Correspondence to: J. Qin, Metallurgy and Materials Science Research Institute, Chulalongkorn University, Bangkok 10330, Thailand.
 E-mail: jiaqianqin@gmail.com

X. Zhang, State Key Laboratory of Metastable Materials Science and Technology, Yanshan University, Qinhuangdao 066004, China.
 E-mail: xyzhang@ysu.edu.cn

a Metallurgy and Materials Science Research Institute, Chulalongkorn University, Bangkok 10330, Thailand

b State Key Laboratory of Metastable Materials Science and Technology, Yanshan University, Qinhuangdao 066004, China

c International Graduate Program of Nanoscience and Technology, Chulalongkorn University, Bangkok 10330, Thailand

co-electrodeposition (SCD) is gaining importance in producing better quality metal matrix composite coatings.^[29] The salient features of SCD technique are higher incorporation of the reinforcements, for lower bath concentrations and higher degree of uniformity of the distribution of particles in the metal matrix. Examples of this technique that have been investigated and fabricated successfully include Si_3N_4 ,^[30] SiC ,^[31,32] Al_2O_3 ,^[11,33] polytetrafluoroethylene,^[34] and diamond,^[35] etc. Among these reported results, they just bent the substrate to 90° and suitably masked to expose an effective plating area. However, the vertical area of substrate in the electrolyte could affect the particle dispersion.

Abi-Akar *et al.*^[36] investigated the effect of gravity on co-deposition of the composite coatings. Uniform surface distribution of particles in the metal matrix is more readily obtained under low-gravity environment. Volume per cent of co-deposited particles is greatly improved for large size particles in low g (45 µm). These particles are difficult to incorporate in the metal when making bench co-depositions. This factor along with the long adsorption time achievable in low g allowed the deposition of large diamond particles. Volume per cent of small particles (<1 µm) is not enhanced by the low-g conditions in comparison to 1 g experiments, while that of 5 µm particles produces similar results to the 1 g controls. In 2007, Pushpavanam *et al.*^[35] prepared the Ni-diamond and Ni-Co-diamond coatings by electrodeposition using sedimentation technique on mild steel substrate. However, they fabricated the diamond composite coating from smaller diamond (6–12 µm) particles. According to Abi-Akar *et al.*^[36] results, the gravity of these smaller diamond particles do not strongly affect the coating, but larger diamond particles (~45 µm) could significantly influence on the diamond content in deposits. Until now, no larger diamond (~45 µm) composite coatings by CED using sediment technique

were reported. Therefore, in the present work, Ni-monolayer diamond particle composite coatings has been fabricated by SCD using the developed setup; the effect of diamond concentration in bath, current density, and bath temperature on Ni-diamond co-deposition has been studied, and their tribological properties were investigated by evaluating the microstructure, surface roughness, wear resistance, and cutting performance.

Experimental

Processing

The Ni-diamond composite coatings were prepared by constant current electrodeposition from a typical Watts bath without any additives. The bath composite and plating conditions are listed in Table 1. Analytical reagents and deionized water were used to prepare the plating solution. The diamond particles of a mean particle size 45 µm (Huanghe Xuanfeng Co. Ltd., China) were chosen to co-deposit with nickel in the present experiments. The concentration of diamond particles in the bath are 1, 3, and 5 g l⁻¹. The pH values of the baths were adjusted to 3.2 using H₂SO₄ or NaOH. Prior to the co-deposition, the carbon steel substrates were polished using SiC (1200 mesh) sand paper and immersing in 10% NaOH solution at 70°C, 14% HCl solution at room temperature, and ultrasonicated in acetone at room temperature for 5 min. The steel substrates were masked with insulated tape to leave 2 × 2 cm² of exposed area. A Pt-coated Fe mesh plate was used as an anode.

The steel substrate and Pt-coated Fe mesh plate with a distance of 40 mm were horizontally immersed into 200 ml of the electrodeposition baths. In this study, we design a simple setup for SCD. Figure 1a shows the designed setup for SCD. The solution was stirred using a magnetic stirrer. Stirring was given initially for 5 min to bring all the diamond powder into the suspension and then stopped. The deposition was continued for 15, 25, and 35 min for current density of 6, 4, and 2 A dm⁻², respectively, to allow the particles to settle on the substrate while the deposition proceeded. Then, one can shake the setup and remove the excess diamond particles. Finally, the same process was repeated to obtain deposit thickness of 35 ± 5 µm. A schematic diagram of the fabrication process used to produce Ni-diamond coatings is shown in Fig. 1b.

In order to show the differences in the wear and cutting performance, conventional co-deposition (CED) was also performed. In addition, a pure nickel coating was also obtained by SCD using the developed setup.

Table 1. Chemical composition of the electrodeposition bath and the operating conditions

Chemical/parameters	
NiSO ₄ ·6H ₂ O	300 g l ⁻¹
NiCl ₂ ·6H ₂ O	45 g l ⁻¹
H ₃ BO ₃	45 g l ⁻¹
Diamond particles	1, 3, and 5 g l ⁻¹
pH	3.2
Temperature	40, 50, and 60 °C
Current density	2, 4, and 6 A dm ⁻²

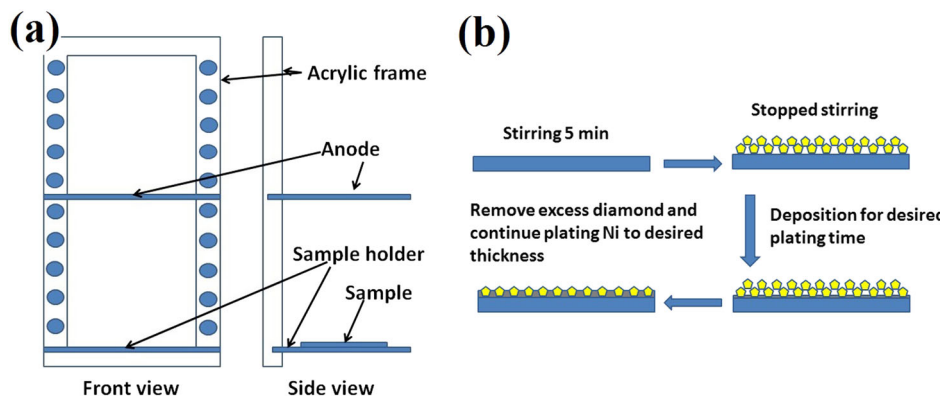


Figure 1. (a) The developed setup for SCD technique and (b) schematic diagram of the deposition process for Ni-diamond composite coatings.

Characterization

Prior to surface analysis, all coatings were washed in deionized water and ultrasonicated in acetone for 5 min. Scanning electron microscopy (SEM) was used to determine the thickness of coating. SEM (Hitachi, S4800) was performed to observe the surface of the coatings. Energy-dispersive X-ray spectroscopy (EDX) was carried out to determine the chemical composition between diamond particles and Ni matrix. In addition, 3D images were also obtained by laser microscope (OLS4000, Olympus). The particle concentration in the composite coatings was evaluated using the gravimetrically method. Deposits were stripped in 50% (v/v) nitric acid, which was filtered, and the mass of diamond powder in the deposit was estimated gravimetrically. The phases of the composite coatings were detected via X-ray diffraction using an X'Pert Pro diffractometer (Panalytical). The surface profile (Gauges, Ambs, USA) was used to measure the surface roughness.

Ball-on-disc tester was performed to study the friction and wear properties of the coatings under dry sliding conditions at room temperature. The upper specimen, with a diameter of 6.3 mm, was a WC (YG8, Zhuzhou Co. Ltd, China) ball bearing with a hardness of 18 GPa and a surface roughness (R_a) of 0.025 μm . All tests were performed under a 2 N load with a rotation speed 200 rpm. The friction coefficient and sliding time were recorded automatically during the test. The coating samples were washed in distilled water and acetone before each test. The weight loss of the coatings after the wear test was measured using an electronic balance with an accuracy of 0.01 mg. In addition, the cutting performance (material removal rates for the corresponding ball bearings) was also evaluated by using the weight loss and the diameter of the wear scar of the ball bearing.

Results and discussion

X-ray diffraction

Ni-diamond composite coatings were successfully co-deposited on steel surfaces with a high concentration and well diamond distribution in deposits by SCD using the new developed setup (Ni-Dia_SCD). Figure 2 shows the XRD patterns of pure Ni and Ni-diamond composite coatings. Figure 2a presents the XRD patterns for Ni-diamond composite coatings prepared with diamond concentration in bath 3 g l^{-1} , current density 2 A dm^{-2} , and at different bath temperatures of 40, 50, and 60 °C. Figure 2b shows the XRD patterns for Ni-diamond composite coatings prepared with diamond concentration in bath 3 g l^{-1} , bath temperature 50 °C, and at different current densities of 2, 4, and 6 A dm^{-2} . All the coatings exhibit two phases of Ni (JCPDS, No. 04-0850) and diamond (JCPDS, No. 65-0537). Pure Ni coatings were also deposited with current density 2 A dm^{-2} and at bath temperature of 50 °C. It reveals that the Ni-diamond composite coatings were successfully fabricated by SCD using the developed setup.

Surface morphology and cross-section observations

Microstructural analysis on the coated surface as well as on the cross section was carried out with SEM. SEM images of the cross-sectional profiles of the Ni-diamond coatings are shown in Fig. 3. Figure 3 shows the typical SEM images of the Ni-diamond coatings prepared with diamond concentration in bath 3 g l^{-1} , bath temperature 50 °C, at different current densities of 2, 4, and 6 A dm^{-2} . From the cross-section SEM images, it shows that the thickness of Ni-diamond coatings is $40 \pm 5 \mu\text{m}$. It can

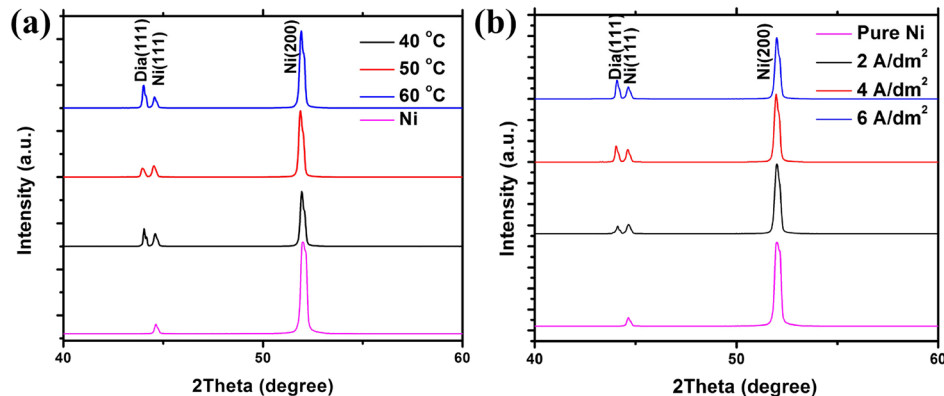


Figure 2. XRD patterns of Ni-diamond coatings prepared with diamond concentration in bath 3 g l^{-1} , and (a) different bath temperatures and (b) different current densities, compared with XRD of pure Ni coating.

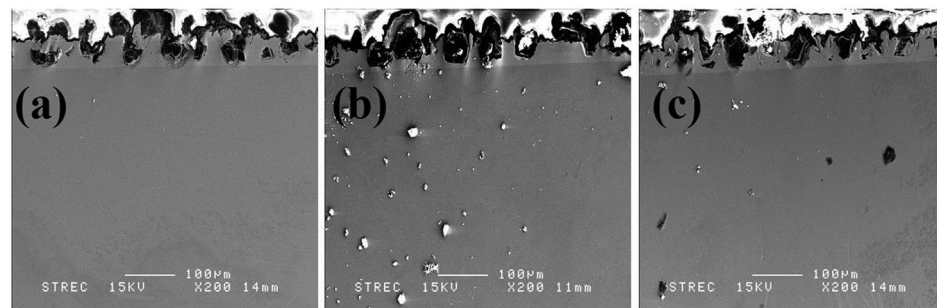


Figure 3. SEM images presenting the cross sections of the Ni-diamond composite coatings prepared with diamond concentration in bath 3 g l^{-1} , bath temperature 50 °C, at different current densities, (a) 2 A dm^{-2} , (b) 4 A dm^{-2} , and (c) 6 A dm^{-2} .

be seen that the black area is diamond particles and the uniform distribution of diamond particles with diameters of 40~50 μm is embedded in the Ni layer.

Figures 4a, 4c, and 4e show the surface morphology of a Ni-diamond coatings fabricated via SCD technique with current

density of 2 A dm^{-2} , bath temperature 50°C , and different diamond concentrations in bath, 1, 3, and 5 g l^{-1} , respectively. Clearly, more diamond particles are embedded in the matrix presented in Fig. 4e than in that shown in Fig. 4a. These SEM micrographs show the uniform distribution of diamond particles throughout the deposits,

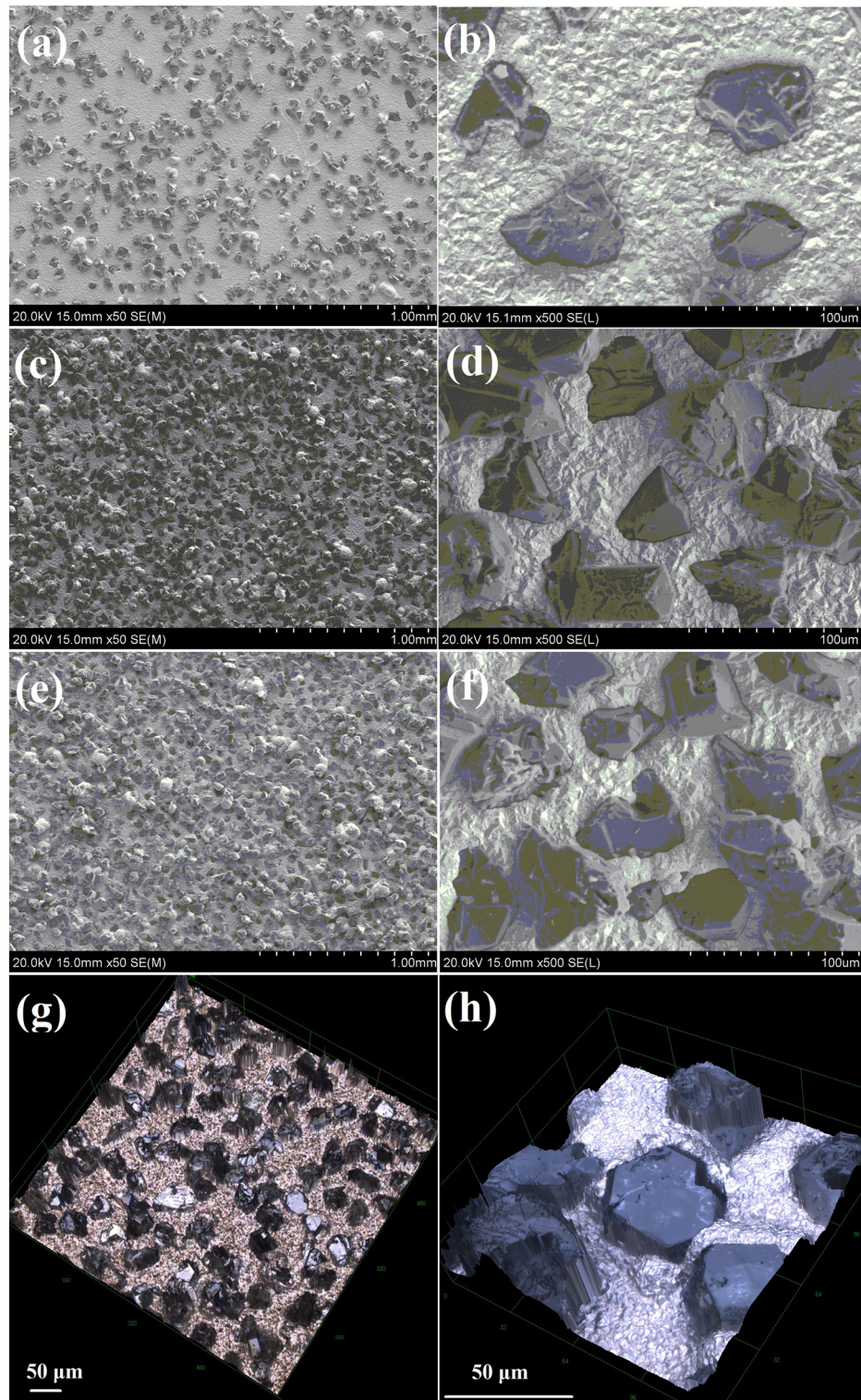


Figure 4. SEM images of a Ni-diamond coatings fabricated via SCD technique with current density of 2 A dm^{-2} , bath temperature 50°C , and different diamond concentrations in bath, (a, b) 1 g l^{-1} , (c, d) 3 g l^{-1} , (e, f) 5 g l^{-1} . (g, h) The typical 3D images of Ni-diamond coatings with the deposition time of current density of 2 A dm^{-2} , bath temperature 50°C , and diamond concentration in bath, 3 g l^{-1} .

and the diamond content in deposits increases with the diamond concentration in bath increasing. Figures 4b, 4d, and 4f show the enlarged SEM images of Figs. 4a, 4c, and 4e, respectively. These enlarged SEM images reveal that the diamond particles were successfully co-deposited in the Ni matrix, not only settled down on the substrate. To confirm the SEM observation, laser microscope was also performed to see the 3D morphology. Figures 4g and 4h show the typical 3D images of the Ni-diamond composite coatings. It can be seen that diamond particles were embedded into the Ni matrix.

Effect of deposition parameters on diamond content in deposits

The diamond content in deposits was measured by gravimetrically method. Figure 4 shows the SEM images of Ni-diamond composite coatings under different diamond concentrations in bath. According to SEM images, the particle incorporation in the deposits for diamond concentration in bath of 5 g l^{-1} is less and the extent of agglomeration of particles is also less. With 5 g l^{-1} , the particle incorporation in the deposits is more, but the extent of agglomeration of particles is also high. This could be caused by the blocking effect of the powder on the surface area available for plating.^[37] Figure 5 shows the effect of diamond concentration in baths on diamond content in deposits. With 1 g l^{-1} , diamond content in deposit was 64.1, 61.3, and 52.9 wt%, with bath temperature of 50°C , current density of 2, 4, and 6 A dm^{-2} , respectively. While the diamond concentration in bath increased up to 5 g l^{-1} , diamond content in deposit was 76.1, 72.1, and 70.8 wt%, with bath temperature of 50°C , current density of 2, 4, and 6 A dm^{-2} , respectively. It can be seen that diamond content in deposits increases with increasing the diamond concentration in bath under all of the current densities (2, 4, and 6 A dm^{-2}). This result is consistent with the SEM-observed trends in different diamond concentrations.

The effect of temperature on diamond contents in deposits was also investigated. Figure 6 shows the summary of the effect of diamond parameters on the diamond contents in deposits with varying the current density. The results show that the diamond content in deposit was 70.6, 69.0, and 62.4 wt%, with bath temperature of 40°C , current density of 2, 4, and 6 A dm^{-2} , respectively.

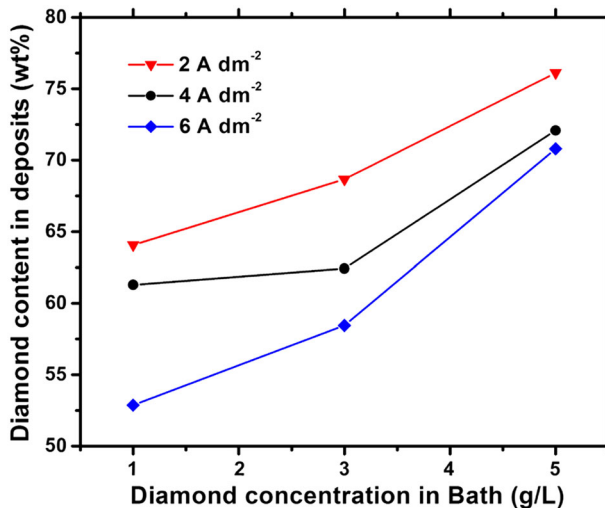


Figure 5. Effect of diamond concentration in the nickel bath on its wt % incorporation in the deposit. pH 3.2, 50°C , current density, ▼ 2 A dm^{-2} , ● 4 A dm^{-2} , ♦ 6 A dm^{-2} .

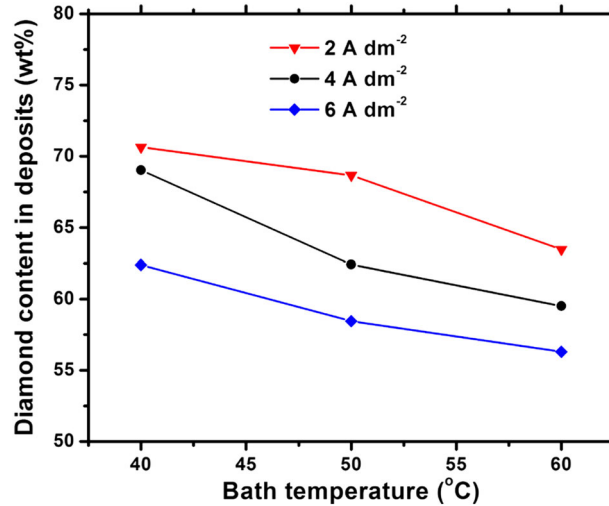


Figure 6. Effect of bath temperature on its wt% incorporation in the deposit. Diamond concentration in bath, 3 g l^{-1} , pH 3.2, current density, ▼ 2 A dm^{-2} , ● 4 A dm^{-2} , ♦ 6 A dm^{-2} .

While the bath temperature increased up to 60°C , diamond content in deposit was 63.5, 59.5, and 56.3 wt%, with current density of 2, 4, and 6 A dm^{-2} , respectively. At high operating temperature, the metal deposition rate increases reducing the volume per cent diamond incorporation.

Figures 5 and 6 also show the effect of current density on the weight percentage incorporation of diamond in the deposits. At the current density of 2 A dm^{-2} , the diamond content in deposit was 70.6, 68.7, and 63.5 wt%, with bath temperature of 40, 50, and 60°C , respectively. While the current density increased up to 6 A dm^{-2} , diamond content in deposit was 62.4, 58.45, and 56.3 wt%, with bath temperature of 40, 50, and 60°C , respectively. Clearly, with increasing current density, the diamond content in deposits decreases. The real current density prevailing at the cathode is considerably higher than the apparent current density in the CED composite coatings, because the exposed area for deposition is reduced by the particles. This condition is more effective in SCD as a result of higher particle incorporation, especially for the larger particles. So, with increasing the current density, the rate of metal deposition increases, and hence, the diamond content decreases.

For comparison, we also deposited pure Ni by SCD and Ni-diamond composite coating using conventional electroplating method (Ni-Dia_CED) (Fig. 7). Figures 7a and 7b show the SEM of the electrodeposition of Ni-diamond composite coatings prepared with current density 2 A dm^{-2} , diamond concentration in bath 3 g l^{-1} , and bath temperature 50°C using the conventional setup. Figure 7c shows the SEM of the Ni coatings. According to the SEM morphology, the new developed SCD setup improves the concentration and distribution of diamond grains significantly.

Effect of deposition parameters on the surface roughness

The average roughness values were approximately $0.22\text{ }\mu\text{m}$ pure Ni coatings, $6.5\text{ }\mu\text{m}$ for the Ni-diamond composite coatings prepared using conventional electrodeposition, and $8\text{--}11\text{ }\mu\text{m}$ for the Ni-diamond composite coatings fabricated by SCD using the new developed setup. Figure 8 shows the surface roughness of Ni, Ni-diamond composite coatings with different deposition parameters. The existence of the diamond particles clearly leads to an increase in the roughness, which should be caused by the increased current

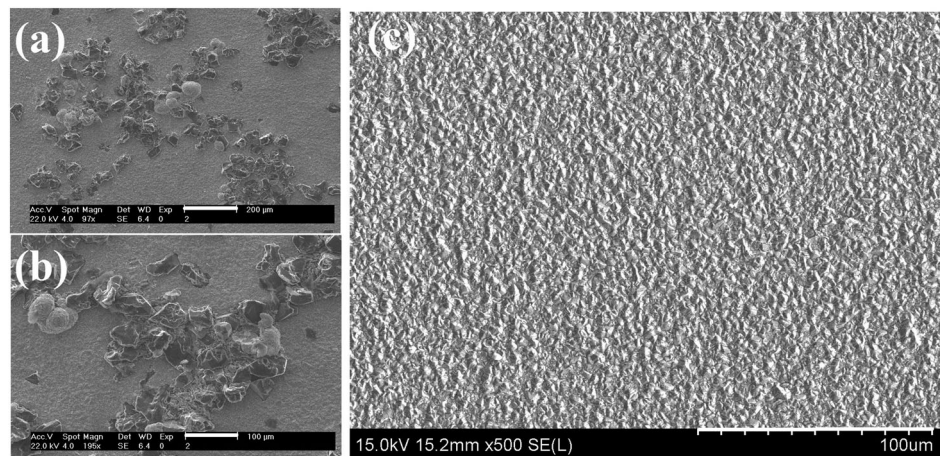


Figure 7. (a) SEM images of the electrodeposition of Ni-diamond composite coatings prepared with current density 2 A dm^{-2} , diamond concentration in bath 3 g l^{-1} , and bath temperature 50°C using the conventional setup. (b) The higher magnification of (a), (c) SEM images of the pure Ni coatings.

density at the substrate surface as a result of the blocking effect of the diamond particles.^[34] The surface roughness of Ni-diamond composite coatings prepared using SCD is larger than that of Ni-diamond composite coatings fabricated using CED. This is also caused by the blocking effect of the more diamond particles in the SCD. Moreover, in the SCD process, there has an increase trend in the surface roughness with increasing the diamond concentration in bath, while the temperature and current density did not give a clearly trend. Because the diamond content in deposits increases with diamond concentration in bath increasing, the surface roughness is higher than those of lower diamond concentration in bath as a result of the strong blocking effect of the diamond particles for the higher diamond concentration in bath.

Tribological performance of the coatings

Figure 9 shows the typical friction curve of the Ni-diamond composite coatings under dry wear conditions. The friction coefficient is approximately 0.15–0.3, while the pure Ni exhibits the highest

friction coefficient of 0.35–0.55. The probable reason for this is that the cutting performance of the Ni-diamond composite coatings is better than those of pure Ni coatings. In addition, the higher diamond contents of coatings exhibit higher friction coefficient; this implies that the distribution density of diamond particles embedded in Ni matrix is also responsible for the friction.

The weight loss of the pure Ni and Ni-diamond composite coatings are presented in Fig. 10, which indicates that the weight loss of coatings increase with increasing diamond content in deposits; the reason for this is that the higher diamond content in deposits could exhibit better cutting performance; hence, the contact area increases quickly with increasing deposition time. The material removal rate of the WC ball bearing is shown in Fig. 11. From Fig. 11, one can see that the removal rate of the WC ball increases with increasing diamond content in the Ni, Ni-Dia_CED, and Ni-Dia_SCD. It is observed that the removal rate of the ball on the Ni-Dia_SCD coatings is ~75 times and ~150 000 times higher than those on the Ni-Dia_CED and pure Ni coatings, respectively. The results imply that Ni-diamond composite coatings prepared using SCD could increase the cutting efficiency significantly.

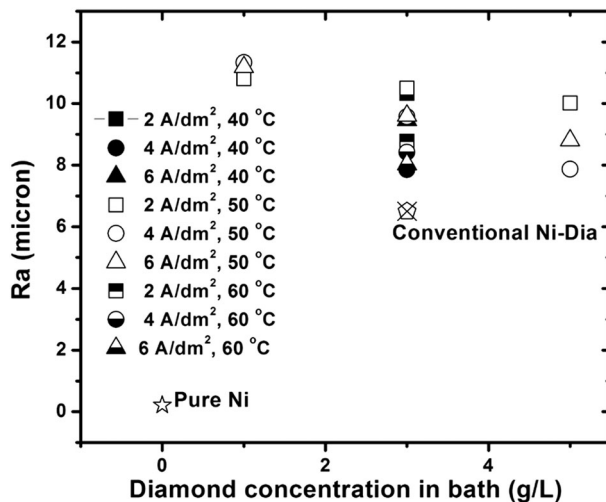


Figure 8. Surface roughness of Ni-composite coating prepared with different deposition parameters by SCD. The surface roughness of pure Ni and Ni-diamond composite coatings prepared with the conventional setup were also shown for comparison.

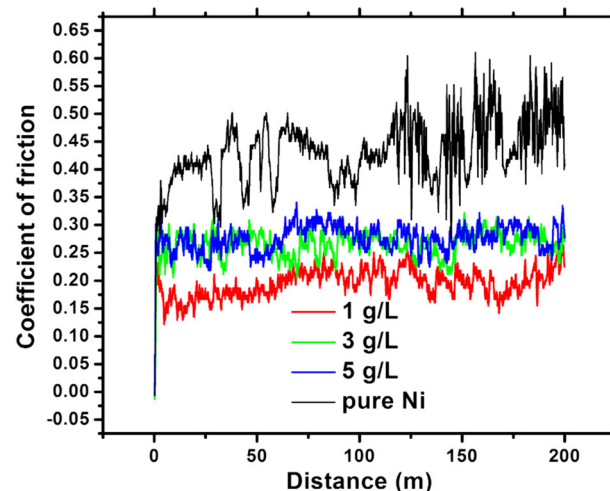


Figure 9. The friction coefficient of Ni-diamond composite coatings prepared with current density 4 A dm^{-2} , temperature 50°C , and different diamond concentrations in bath, $1, 3$, and 5 g l^{-1} . The friction coefficient of pure Ni coatings was also added for comparison.

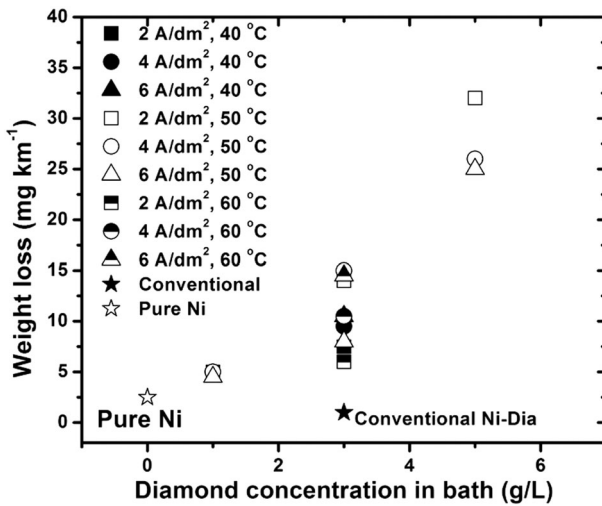


Figure 10. The weight loss of Ni-diamond composite coatings fabricated by SCD, Ni-diamond composite coatings prepared by CED, and pure Ni coatings.

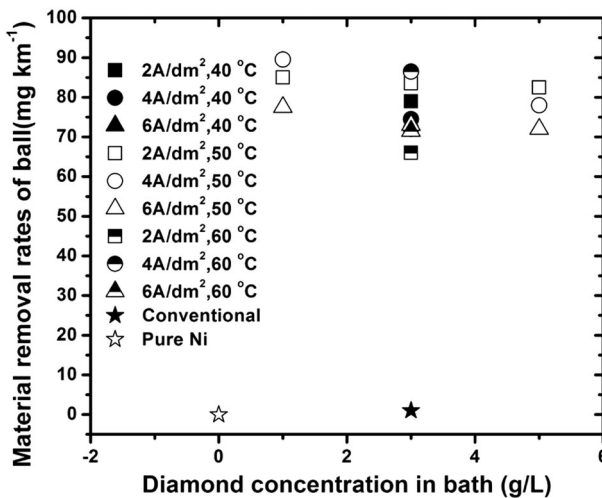


Figure 11. The WC material removal by the corresponding Ni-dia_SCD, Ni-dia_CED, and pure Ni coatings.

Because the weight loss of Ni-Dia_SCD is larger than those of Ni-Dia_CED and pure Ni coatings, one cannot evaluate the wear resistance using the weight loss value in the present study. Therefore, a new parameter η is introduced. Here, η is the ratio of weight loss of coatings to weight loss of WC ball bearing (weight loss of coatings / weight loss of WC ball bearing), the smaller η means better wear resistance. Figure 12 gives the relationship of the ratio η under different deposition parameters. The comparison between Ni-diamond composite coatings and pure Ni coatings clearly indicated that the anti-wear performance is drastically improved by adding diamond particles. Among the composite coatings, it is seen that the wear resistance for Ni-Dia_SCD coatings are approximately the same, but it is higher than those of Ni-Dia_CED coatings.

The improved wear resistance and cutting performance of the Ni-diamond composite coatings prepared using SCD methods can also be confirmed using the optical microscope (OM) images of the wear surface of coatings and WC ball bearing depicted in Fig. 13. Figure 13 shows the typical OM images of the wear scar for the Ni-dia_SCD coatings, Ni-dia_CED coatings, and pure Ni

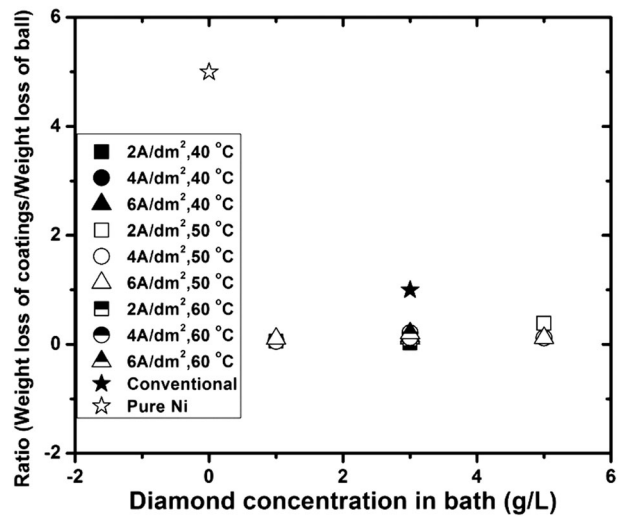


Figure 12. The ratio of weight loss of coatings to WC ball bearing at different deposition parameters.

coatings. It is observed that the wear scar area for both Ni-diamond coatings and WC ball is larger than those of pure Ni coatings and the corresponding WC ball. Furthermore, the wear scar area for Ni-dia_SCD coatings and WC ball is larger than those of Ni-dia_CED coatings and the corresponding WC ball. Therefore, it is understandable for higher weight loss of Ni-dia_SCD coatings.

Figure 14 shows the SEM and OM images of the worn surface of the Ni-dia_SCD coatings and pure Ni coatings. As illustrated in Fig. 14a, it can be seen that before and after wear testing zone was the same, no peeled off diamond particles were found during the wear testing. As indicated in Figs. 3 and 14a, the suitable exposed diamond particles are responsible for the removal of WC material from the ball bearing, and the Ni matrix can strongly hold the diamond particles. However, for the pure Ni coatings, distinct scratches, delaminations, and some plastic deformations are found along the wear track, and heavy peeling occurs in the bulk (refer to Fig. 14b), indicating a possible adhesive wear mechanism. To determine the interface of chemical bonding and composition between the diamond particles and Ni matrix, the elemental analysis between diamond and Ni was also performed by EDX. Figures 14c and 14d show the EDX analysis for the surface and cross section, respectively. Here, line scans EDX through the diamond particle zone and Ni zone. From the EDX results, it can be seen that Ni zone only showed the Ni spectrum and diamond particle zone only presented the carbon spectrum. Thus, it revealed that diamond particles adhere to steel surface only by mechanical interlocking with Ni plating.

The wear resistance and cutting performance of Ni-dia_SCD coatings is superior to those of the Ni-dia_CED coatings, as a result of not only the content but also the distribution in which the diamond particles are incorporated within the Ni matrix. For the Ni-Dia_SCD coatings, one can see that the diamond particles are tightly held and strongly bonded within the diamond particles for all of the samples. However, with increasing the diamond content in deposits, the space between diamond and diamond embedded in the Ni matrix decreases (refer to Fig. 4). Because diamond is far harder than WC ball, the exposed diamond particles act as many small cutters to enhance material remove. During the wear testing, the removed WC material was located in the space between diamond and diamond embedded in the Ni matrix, so the suitable space could further improve the cutting efficiency. This is why the cutting performance decreases with increasing the diamond

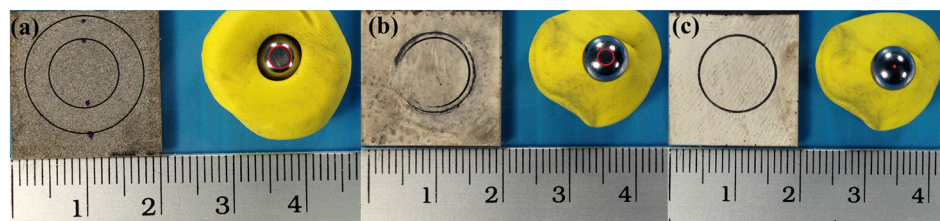


Figure 13. The typical OM images of wear surface for coatings and corresponding WC ball bearing. (a) Ni-dia_SCD composite coatings, after wear testing, no difference was found. The circle marker is the possible wear track. The wear process removed big parts of WC ball, and it could not continue. (b) The clearly wear track on Ni-dia_CED composite coatings. During the same wear testing time, the corresponding weight loss of WC ball was lower than those of Ni-dia_SCD. (c) The clearly wear track on pure Ni coatings. The pure Ni coatings only removed a point from the WC ball bearing.

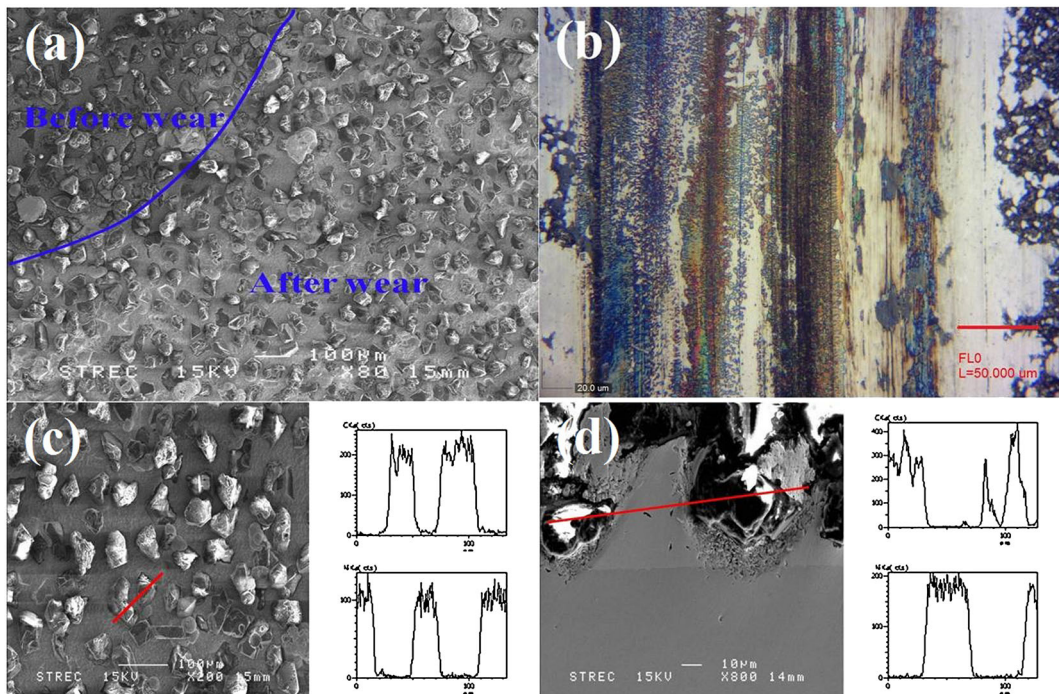


Figure 14. SEM and OM images of the worn coating surfaces under dry sliding conditions: (a) Ni-dia_SCD, (b) pure Ni coatings, (c) EDX analysis of worn surface, and (d) EDX analysis of cross section of composite coating.

content in deposits for the Ni-Dia_SCD coatings. As shown in Fig. 15, the wear resistance of the Ni, Ni-dia_CED, and Ni-Dia_SCD coatings as a function of the diamond content in deposits was also plotted. As indicated in Fig. 15, wear resistance increases with diamond content in deposits increasing for Ni, Ni-dia_CED, and Ni-Dia_SCD coatings. However, for Ni-Dia_SCD coatings, an approximately the same in wear resistance occurs with an increase in diamond content below 72 wt% while further increases in diamond content result in a rapid decrease in wear resistance. With lower diamond content in deposits, although the particle incorporation in the deposits is less, the extent of agglomeration of particles is also less. With higher diamond content, the particle incorporation in the deposits is more, but the extent of agglomeration of particles is also high. Moreover, also, some diamond particles were not well embedded in the Ni matrix (refer to Fig. 4). This could be caused by the blocking effect of the powder on the surface area available for plating.^[37] Moreover, the cutting performance decreases with the diamond content increasing (refer to Fig. 11), this reveals that the more diamond particles of composite coatings are not sure, the better wear resistance and cutting performance.

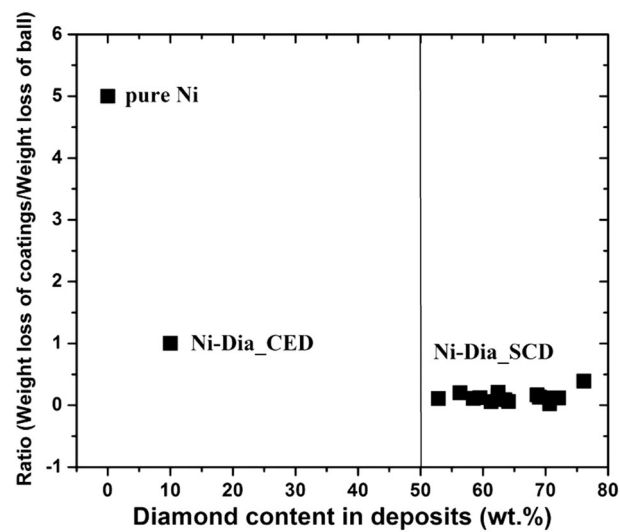


Figure 15. The wear resistance of the Ni, Ni-Dia_CED, and Ni-Dia_SCD coatings as a function of the diamond content in deposits.

Conclusion

Sediment co-deposition is a suitable technique for producing composite coatings with high particle concentration and better distribution of particles. In the present study, we designed a facile setup for SCD technique. The monolayer Ni-diamond composite coatings with high particle content and uniform distribution of large diamond particles ($\sim 45\text{ }\mu\text{m}$) were successfully prepared by SCD using this developed setup with different deposition parameters. With adding diamond particles, the wear resistance and cutting performance are drastically improved. For the composite coatings, the anti-wear and cutting performance of Ni-dia_SCD coatings is higher than those of Ni-dia_CED coatings. In the SCD process, with the increasing diamond content, the wear resistance is approximately the same, and the cutting performance decreases. Therefore, not only the diamond particles content is responsible for the wear resistance and cutting performance, the distribution of diamond particles is also very important factor. The suitable diamond content and space between diamond and diamond are the key factors for wear resistance and cutting performance.

Acknowledgements

This research is supported by the Ratchadaphiseksomphot Endowment Fund of Chulalongkorn University (RES560530022-AM). J.Q. would like to acknowledge the support from support from Ratchadaphisek Somphoch Endowment Fund (2013), Chulalongkorn University (CU-56-805-FC), National Research University Project, Office of Higher Education Commission (WCU025-AM57), Thailand Research Fund (TRG5780222), Ratchadapisek Somphoch Endowment Fund for new faculty of Chulalongkorn University, and Key Laboratory of Metastable Materials Science and Technology, Yanshan University. J.Q. Y.B. A.T. would like to acknowledge the support from Ratchadapisek Somphoch Endowment Fund, Chulalongkorn University, granted to the Surface Coatings Technology for Metals and Materials Research Unit (GRU 57-005-62-001). X.Z. M.M. R.L. would like to acknowledge the support from NBRPC (grant 2013CB733000), NSFC (grants 51271161/51171160/51002130/51171163).

References

- [1] C. T. J. Low, R. G. A. Wills, F. C. Walsh, *Surf. Coat. Tech.* **2006**, 201, 371–383.
- [2] L. Benea, P. L. Bonora, A. Borello, S. Martelli, F. Wenger, P. Ponthiaux, J. Galland, *J. Electrochem. Soc.* **2001**, 148, C461–C465.
- [3] A. F. Zimmerman, G. Palumbo, K. T. Aust, U. Erb, *Mater. Sci. Eng. A* **2002**, 328, 137–146.
- [4] K. H. Hou, M. D. Ger, L. M. Wang, S. T. Ke, *Wear* **2002**, 253, 994–1003.
- [5] P. Gyftou, M. Stroumbouli, E. A. Pavlatou, P. Asimidis, N. Spyrellis, *Electrochim. Acta* **2005**, 50, 4544–4550.
- [6] E. A. Pavlatou, M. Stroumbouli, P. Gyftou, N. Spyrellis, *J. Appl. Electrochem.* **2006**, 36, 385–394.
- [7] S.-C. Wang, W.-C. J. Wei, *Mater. Chem. Phys.* **2003**, 78, 574–580.
- [8] D. K. Singh, V. B. Singh, *J. Electrochem. Soc.* **2011**, 158, D114–D118.
- [9] M.-D. Ger, *Mater. Chem. Phys.* **2004**, 87, 67–74.
- [10] F. Hou, W. Wang, H. Guo, *Appl. Surf. Sci.* **2006**, 252, 3812–3817.
- [11] Q. Feng, T. Li, H. Yue, K. Qi, F. Bai, J. Jin, *Appl. Surf. Sci.* **2008**, 254, 2262–2268.
- [12] H. Güll, F. Kılıç, S. Aslan, A. Alp, H. Akbulut, *Wear* **2009**, 267, 976–990.
- [13] N. K. Shrestha, D. B. Hamal, T. Saji, *Surf. Coat. Tech.* **2004**, 183, 247–253.
- [14] K. Krishnaveni, T. S. N. Sankara Narayanan, S. K. Seshadri, *J. Alloy. Compd.* **2008**, 466, 412–420.
- [15] E. C. Lee, J. W. Choi, *Surf. Coat. Tech.* **2001**, 148, 234–240.
- [16] H. Ogihara, M. Safuan, T. Saji, *Surf. Coat. Tech.* **2012**, 212, 180–184.
- [17] W.-H. Lee, S.-C. Tang, K.-C. Chung, *Surf. Coat. Tech.* **1999**, 120–121, 607–611.
- [18] T. W. Tomaszewski, *Trans. Inst. Met. Finish.* **1976**, 54, 45–48.
- [19] L. Wang, Y. Gao, H. Liu, Q. Xue, T. Xu, *Surf. Coat. Tech.* **2005**, 191, 1–6.
- [20] C. S. Lin, K. C. Huang, *J. Appl. Electrochem.* **2004**, 34, 1013–1019.
- [21] L. Chen, L. Wang, Z. Zeng, J. Zhang, *Mater. Sci. Eng. A* **2006**, 434, 319–325.
- [22] A. Hovestad, L. J. J. Janssen, *J. Appl. Electrochem.* **1995**, 25, 519–527.
- [23] D. Lee, Y. X. Gan, X. Chen, J. W. Kysar, *Mater. Sci. Eng. A* **2007**, 447, 209–216.
- [24] L. Chen, L. Wang, Z. Zeng, T. Xu, *Surf. Coat. Tech.* **2006**, 201, 599–605.
- [25] A. Hovestad, R. J. C. H. L. Heesen, L. J. J. Janssen, *J. Appl. Electrochem.* **1999**, 29, 331–338.
- [26] N. Guglielmi, *J. Electrochem. Soc.* **1972**, 119, 1009–1012.
- [27] J. P. Celis, J. R. Roos, C. Buelens, *J. Electrochem. Soc.* **1987**, 134, 1402–1408.
- [28] C. Riley, H. Abi-Akar, B. Benson, G. Maybee, *J. Spacecraft Rockets* **1990**, 27, 386–390.
- [29] M. Viswanathan, K. S. G. Doss, *Met. Finish.* **1972**, 70, 83.
- [30] C. S. Ramesh, S. K. Seshadri, *Wear* **2003**, 255, 893–902.
- [31] M. Viswanathan, *Met. Finish.* **1973**, 71, 38–43.
- [32] M. Ghose, M. Viswanathan, E. G. Ramachandran, *Met. Finish.* **1980**, 78, 31–35.
- [33] Q. Feng, T. Li, H. Teng, X. Zhang, Y. Zhang, C. Liu, J. Jin, *Surf. Coat. Tech.* **2008**, 202, 4137–4144.
- [34] R. Balaji, M. Pushpavanam, K. Y. Kumar, K. Subramanian, *Surf. Coat. Tech.* **2006**, 201, 3205–3211.
- [35] M. Pushpavanam, H. Manikandan, K. Ramanathan, *Surf. Coat. Tech.* **2007**, 201, 6372–6379.
- [36] H. Abi-Akar, C. Riley, G. Maybee, *Chem. Mater.* **1996**, 8, 2601–2610.
- [37] A. E. Marlborough, *Met. Finish.* **1997**, 95, 22.